Chapter 4

Preparation, characterization, *in-vitro* and *in-vivo* pharmacokinetic evaluation of dimethyl fumarate cocrystals with acid-based coformers

4 Preparation, characterization, *in-vitro* and *in-vivo* pharmacokinetic evaluation of dimethyl fumarate cocrystals with acid-based coformers

4.1 Introduction

Dimethyl fumarate (DMF), a fumaric acid derivative, has been extensively used for the management of psoriasis since 1990 by both oral and topical routes. DMF has been an established and FDA-approved drug for multiple sclerosis (MS) management, owing to its antioxidant-mediated immune modulation effect [182]. It is available as a white crystalline powder that sublimates at a relatively low temperature [70]. This incurs an in-process limitation, as when processed conventionally, about 15-20% of DMF is lost from the final formulation. It occurs most likely because of sublimation during production. Sublimation occurs due to low measurable vapor pressure (Guzowski, John, William Kiesman, and Erwin Irdham. "Process for preparing high purity and crystalline dimethyl fumarate." U.S. Patent No. 9,422,226. 23 Aug. 2016.) also leads to loss of DMF during long-term storage from bulk and its formulations as well [183]. Scientists have tried to tackle the sublimation problem by precoating the API, and some have been attempting to increase the particle size to make it thermostable. Still, these methods put numerous additional unit operations and economic burdens on the formulation development process. Cocrystallization can modulate the physicochemical properties without much change in pharmacological activity. Therefore, we propose to form cocrystals of DMF to address the problem of sublimation. The improvements in physicochemical properties (i.e., melting point, solubility, stability, permeability, bioavailability, tabletability, etc.) can be achieved through various solid dosage forms of an API, which includes the formation of polymorphs, cocrystals, salts, solvates, and many others [184]. Among all the mentioned approaches, cocrystallization has received much interest in pharmaceutical development over recent decades, and it has emerged as a powerful tool capable of modulating the physicochemical properties of different formulations. Many studies have demonstrated

the impact of cocrystallization on the solubility, permeability, and dissolution rate of poorly water-soluble drugs [185].

Hydrogen bond-based design of molecular networks has emerged as a powerful tool in discovering cocrystals [126]. As hydrogen bonds rely on hydrogen bond donor and acceptor characteristics of the functional groups, coformers are selected cautiously based on the nature of API. It is also essential to establish whether a reaction between an API and coformer will result in a cocrystal or salt formation [127]. DMF has four hydrogen bond acceptors measured using Cactvs 3.4.6.11 (PubChem release 2019.06.18), which makes it a potential molecule to undergo cocrystallization. Cocrystals of DMF with gentisic acid and camphoric acid have been reported to show enhanced absorption and bioavailability [130]. Citric acid has four hydrogen bond donor counts determined by Cactvs 3.4.6.11 (PubChem release 2019.06.18). It has been a choice of coformer for making numerous cocrystals [186]. Succinic acid has two hydrogen bond donors and four acceptor counts calculated by Cactvs 3.4.6.11 (PubChem release 2019.06.18). It is an efficient coformer extensively used for cocrystallization [187].

DMF is a prodrug with monomethylfumarate (MMF) as its primary metabolite [138], many studies have shown DMF to exert more cytoprotective effect than MMF [139]. Once Absorbed DMF/MMF rapidly penetrates blood cells, mainly peripheral blood mononuclear cells (PBMC), and covalently binds to GSH and other molecules [111]. PBMC analysis is one of the important parameters to evaluate the pharmacological actions of DMF, and LPS-induced inflammation in PBMC has been utilized in this work to assess the anti-inflammatory activity of DMF and formulated cocrystals [140]. Moreover, DMF is well known to decrease the synthesis of pro-inflammatory mediators like TNF-α, IL-1β, ROS, and IL-6 in activated microglia and astrocytes and LPS-

activated PBMCs [141]. To ascertain any change in biological or pharmacological activity, we have evaluated the effect of DMF and the cocrystals on changes in intracellular ROS, TNF-α, and IL-6 activity in LPS-induced PBMC.

The cocrystallization approach is a reliable method to modulate the physicochemical properties of drug molecules. Low thermostability-based sublimation-mediated loss of DMF has motivated us to formulate its cocrystals. For the first time, DMF cocrystals have been formulated to tackle its thermostability problem. We have characterized the cocrystals using thermal stability indicators such as DSC, TGA, and thermal assault. Spectral tools like FTIR and PXRD further support cocrystallization. To evaluate the thermostability of the cocrystals, we have exposed DMF and the formulated cocrystals to an extreme condition of 60°C and 75% RH for 20 days. We have compared DMF and its formulated cocrystals for *in-vitro* cytotoxicity LPS-induced alterations in ROS, IL-6, and TNF-α in PBMC. We have also performed *in-vitro* dissolution and *in-vivo* pharmacokinetic profiling of DMF with the cocrystals.

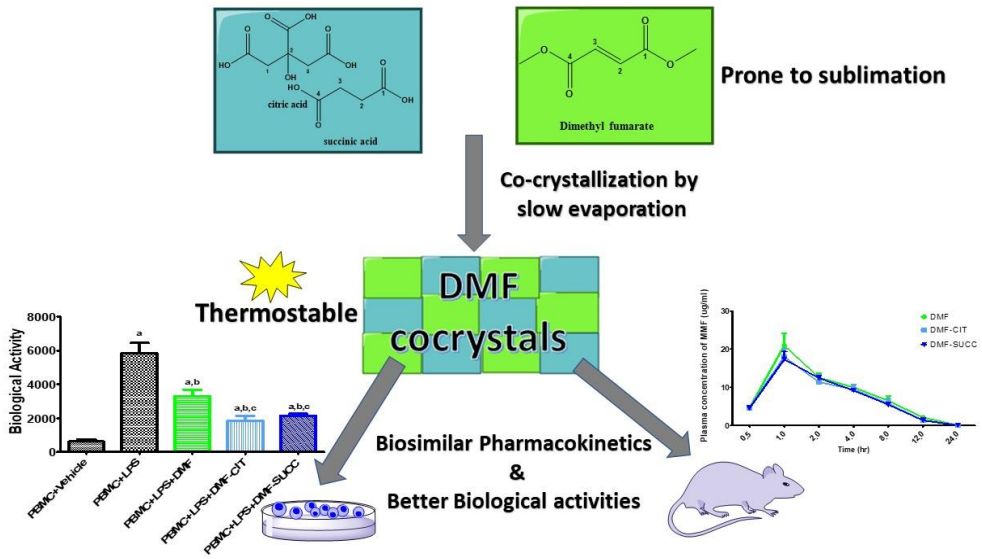

Figure 4-1 Graphical outline

4.2 Materials and methods

4.2.1 Molecular docking

The structures of succinic acid, citric acid, and dimethyl fumarate were sketched through Chemdraw 15. These three-dimensional structures were obtained through energy minimization using MMFF94s force field in mol2 file format. These mol2 files were processed and converted to pdbqt using Autodock tools 1.5.6. Autogrid 4.0 was used to calculate grid maps of interaction energies with various types of atoms present (A, C, HD, NA, N, OA, S). The grid box size was set to 40 × 40 × 40 with a grid spacing of 0.375 Å. The grid centered around coordinates (x, y, and z) 0.423, 0.316, and 0.0. The docking was performed by Autodock 4.2.6 using Lamarckian Genetic Algorithm with 10 runs, 150 population sizes, 2,500,000 maximum number of energy evaluations, and 27,000 maximum number of generations. The docked structure was visualized by using Discovery Studio 2020 [144].

4.2.2 Molecular dynamics

The obtained ligand poses were parameterized through Antechamber toolkit using general AMBER force field (GAFF2) and the Austin model with bond and charge correction (AM-BCC1) atomic partial +charges. The topologies and coordinates for the complex of DMF with each SUCC and CIT were built using tleap module of AMBER 20. It was hydrated with TIP3P water molecules in a cubic box with a cut-off distance of 12 Å and neutralised by adding Na^+ and Cl^- ions. The systems were subjected to energy minimisation, heating, density equilibration and equilibration under periodic boundary conditions. The final 5 ns MD productions were carried out at 310.15 K as an NPT ensemble. Further, the post-MD processing was carried out using cpptraj [148].

4.2.3 Experimental animals

Inbred male Sprague Dawley rats weighing 150−200 g (8 to 10 weeks old), were procured from Central Animal House, Institute of Medical Science (IMS-BHU). The experiments were performed by adopting guidelines (NIH publication number 85-23, revised 2015) and approved by the Institutional Animal Ethical Committee, Banaras Hindu University (BHU; Dean/2019/CAEC/1649). Animals were acclimatized in the experimental lab before using them for experiments for a period of one week of acclimatization under standard laboratory conditions (22 ± 2 °C, 12 h light/dark cycle, and relative humidity of 50 ± 5%).

4.3 Materials

DMF was obtained from Disto Pharmaceuticals (Hyderabad-India) as a gift sample, citric acid, succinic acid, and sodium chloride were purchased from Merck (USA), MTT was obtained from SRL chemicals, Hisep was purchased from Himedia, LPS (E. coli, L3129), MMF, dichlorofluorescin diacetate, trypan blue and antibiotics were obtained from Sigma Aldrich, RPMI-1640 and FBS were obtained from Lonza, TNF-α and IL-6 ELISA kits were purchased from Krishgen Biosystems. Ultrapure water was prepared using a Milli-Q ultrapure purification system (Millipore, USA). Countess™ cell counting chamber slides were purchased from Thermo Fisher Scientific. All other chemicals and reagents of high-performance liquid chromatography (HPLC) and analytical grade were procured from local suppliers.

4.3.1 Method of preparation

The solvent evaporation method was used to prepare the cocrystals with the coformers selected by autodocking studies (discussed later). The two cocrystals were formulated by the solvent evaporation method [149]. For making cocrystal DMF and the coformers were

taken in a 1:1 ratio and dissolved separately in ethanol and water, respectively. The individual conformer solution was added dropwise into the DMF solution. The solutions were filtered through a 0.22 µm membrane filter to get a clear homogenous solution and covered with aluminum foil with small openings to facilitate solvent evaporation. They were incubated at 40°C for slow solvent evaporation to obtain cocrystals. The resulting products were dried in an oven at 60 °C overnight to remove any residual solvent and then the cocrystals were gently grounded to a fine powder for further analysis. Finally, physical mixtures were also prepared for both by mixing the constituents in a 1:1 ratio for both in the mortar and pestle.

4.3.2 Attenuated total reflectance FTIR (ATR- FTIR) spectroscopy

FTIR spectra in the region of 600–4000 cm^{-1} were obtained using a Shimadzu IR-Prestige-21 FTIR spectrometer coupled with a horizontal Golden Gate MKII single-reflection ATR system (Specac, Kent, UK) equipped with ZnSe lenses after appropriate background subtraction. The spectral region was set from 400 to 4000 cm^{-1}. All the spectral data were collected at ambient temperature.

4.3.3 Powder X-ray Diffraction (PXRD)

PXRD analysis was conducted by a MiniFlex II benchtop X-ray diffractometer at 30 kV and 15 mA with a Ni-filtered Cu KR radiation source (λ) 1.54 Å) (Rigaku, The Woodlands, TX, U.S.A.). The samples were scanned from 5° to 30° (2θ) at a scanning rate of 0.5°C per min. The diffractograms were processed using Origin Pro.

4.3.4 Thermal analysis

A high melting point demonstrates the thermodynamic stability of the new materials, i.e., the thermal stability of an API can be increased by selecting the coformer with the higher

melting point. The most commonly used techniques for the determination of melting point and thermal stability analysis are thermal gravimetric analysis (TGA) and differential scanning calorimetry (DSC) [151].

4.3.5 Differential Scanning Calorimetry (DSC)

DSC was performed on a DSC-60 Plus Shimadzu differential scanning calorimeter. Accurately weighed samples (4-7 mg) were placed in hermetically sealed aluminium pans and scanned from 25 to 250°C at 10°C/min under a nitrogen purge. The DSC calibration was done using a single-point method with the extrapolated onset of the melting point of a 0.275 mg indium sample.

4.3.6 Thermogravimetric Analysis (TGA)

The decomposition temperature for each substance was determined using a Shimadzu Corporation TGA-50 thermo-gravimetric analyzer. Approximately (4-7 mg) amount of the sample was heated from 25 to 250 °C at a 10°C/min rate. A purge of dry nitrogen (flow rate sample, 60 ml/min; flow rate balance, 40 ml/min) was maintained through the sample chamber during all the experiments to keep an inert environment and to avoid any oxidation of samples.

4.3.7 Evaluation of Sublimation behavior

The sublimation behavior of DMF and the cocrystals were evaluated by following the method of physical stability with some modifications [153]. A known amount of DMF, cocrystals and their physical mixtures were prepared by gentle trituration of the DMF and the respective coformers. The samples contained the exact quantities of DMF in all the glass vials. The mouth of the glass vials was covered with perforated aluminum foil. These glass vials were maintained in an incubator at 60°C,75% RH for 20 days. As

approximately 80% of DMF sublimed by the 20th day, it was not kept in this condition for more than 20 days. Relative humidity was maintained using a saturated solution of sodium chloride kept in a beaker in the same incubator [154]. %DMF sublimed was analyzed after 10 and 20 days, respectively, from the day it was kept in the incubator. To avoid any error due to changes in weight due to the absorption of moisture during the storage period, samples stored were firstly dried in a desiccator under negative pressure at room temperature before performing an assay [188].

4.3.8 *In-vitro* dissolution study

Dissolution was carried out following the method as per FDA (www.accessdata.fda.gov/scripts/cder/dissolution) 100 mg each of DMF and various cocrystals were filled into empty capsule shells and taken into 500 ml phosphate buffer (pH 6.8) at the beginning of the dissolution experiments. The mixtures in the dissolution tester were stirred at 37 °C and 100 rpm. At each time interval, 5 ml of the solution was withdrawn from the instrument and replaced by an equal volume of buffer to maintain the sink condition in the experiment. The collected sample solution was filtered through a 0.22 μm nylon filter, and DMF concentrations were analyzed using HPLC.

4.3.9 Quantification of the drug in prepared cocrystals

DMF quantification was performed by HPLC using Agilent technologies HPLC, Infinity 1260 II equipped with a degasser, a quaternary pump, and an autosampler. 20A3), The system includes a diode array detector and a computer running Agilent open LAB CDS control panel help software for data acquisition and processing. Chromatographic separation was performed at 25±1°C by using a C8 column (4.6 X 250 mm, 5 μm) preceded by a guard column of the same packing material. The mobile phase consisted of acetonitrile and water (80:20). The flow rate was set at 1.0 ml/min, and the total sample

acquisition time was 10 min. Based on previous studies, the UV detector was set at 220 nm, and the injection volume was set at 10µl. For MMF quantification, the solvent system was methanol: potassium phosphate buffer supplemented with 5 mM tetrabutylammonium dihydrogen phosphate 20: 80 (v/v) with a detector set at 215 nm [155].

4.3.10 Isolation and counting of peripheral blood mononuclear cells (PBMCs)

To measure the effect of DMF and its cocrystals on PBMC, blood was obtained from a Sprague Dawley rat through the terminal method (cardiac puncture) and taken into EDTA vacutainer tubes. It was diluted with an equal volume of PBS. Mononuclear cells were separated from peripheral blood samples according to the method described with modification [17]. Briefly, 3 ml of blood mixture was gently layered over 2 ml of Hisep (Ficoll®) solution and centrifuged at 1000 g for 25 min. The white band of mononuclear cells was collected and washed thrice with RPMI 1640 culture medium by centrifugation at 1000 g for 5 min. PBMCs were resuspended in complete RPMI 1640 culture medium (RPMI 1640 medium containing 25 mM HEPES, 2 mM L-glutamine, 10% heat-inactivated fetal calf serum, penicillin (100 U/ml) and streptomycin (100µg/ml)) and adjusted to 2×10^6 cells/ml. After isolating the PBMC, 10 µl aliquots of the sample were mixed with 10 µl of trypan blue (0.4%) (Invitrogen, Italy). It was put into a Countess™ cell counting slides, and the count was made by a Countess® automated cell counter (Invitrogen, Italy) [157].

4.3.11 Cytotoxicity assay

MTT assay was performed to evaluate the cytotoxicity of cocrystals when compared with the pure DMF following [158] with slight modifications. MTT dye, via reductive cleavage of its tetrazolium ring, is converted to purple water-insoluble formazan in the

presence of mitochondrial succinate dehydrogenase in living cells. Thus, the assay signifies the ability of metabolically active cells to reduce MTT to formazan. In other words, the amount of formazan produced serves as a direct indicator of the number of viable cells in the sample. 100 µl aliquot of PBMC containing (approximately 2,00,000 cells) was taken in RPMI-1640 containing 20% FBS taken in a microculture well. 20 µg/ml and 10 µg/ml of cocrystals and DMF respectively, were added into the microculture wells. Blank and vehicle control groups were taken. The culture plate was incubated for 12 hours at 37°C in 5% CO2 condition in the incubator chamber. 10 µl of MTT (5 mg/ml) was added into the microculture wells and again kept for 2 hours at 37°C and 5% CO_2 condition in the incubator. 100 µl of DMSO was added to it and kept again for 2 hours. The absorbance was taken at 570 nm.

4.3.12 Cytokine analysis

Evaluation of cocrystals on LPS-induced PBMC following [159] with slight modifications. PBMC ($2X10^6$ cells/ml) were separated from each rat, and 100 µl aliquot of PBMC containing (approximately 2,00,000 cells) was incubated with and without LPS (10 µg/ml) in 100 ul RPMI containing 20% FCS for 24 hr in a humidified atmosphere of 5% CO_2 at 37 ºC. Later it was washed twice with PBS and incubated with DMF and various cocrystals containing an equivalent of 10 µg/ml DMF for 12 hours. It was washed twice again with PBS. Further, it was incubated for 2 hr with RPMI Containing 20% FCS. It was centrifuged at 1500 g for 5 minutes to obtain a clear supernatant. IL-6 and TNF-α levels in the supernatant were determined using commercial enzyme-linked immunosorbent assay (ELISA) kits following the prescribed method as per the instruction manual.

4.3.13 Measurement of intracellular ROS (i-ROS)

Intracellular ROS (i-ROS) was detected using DCFH-DA, which crosses cell membranes and gets hydrolyzed into nonfluorescent DCFH by intracellular esterases. However, DCFH is oxidized to a highly fluorescent dichlorofluorescein (DCF), in the presence of ROS, which is readily detectable by fluorescence-based instruments like FACS or spectrofluorometer. Intracellular ROS were measured in the PBMC treated with LPS, and further, DMF and its respective cocrystals were evaluated against LPS using the following method [160]. PBMC were counted for total viable cells by trypan blue exclusion assay with the help of Countess™ II automated cell counter. 100 µl aliquot (2 X 10^5 cells) was incubated with LPS (10 µg/ml) in 100 µl RPMI containing 20% FCS for 24 h in a humidified atmosphere of 5% CO_2 at 37 ºC. Later it was washed twice with PBS and incubated with 10 µg/ml DMF and various cocrystals containing equivalent 10 µg/ml DMF for 12 hours. It was washed twice again with PBS. i-ROS were labeled by incubating cells in 100 µl of 20 mM dichlorofluorescein diacetate (DCFH-DA) for 45 min at 37 °C temperature in the dark. After incubation, fluorescence intensity was monitored by using a fluorescence spectrometer (λex: 490 nm; λem: 515 nm).

4.3.14 Pharmacokinetic study

Pharmacokinetic data of DMF and its cocrystals were evaluated in male Sprague Dawley rats weighing 150−200 g (8 to 10 weeks old), following the method [162]. Animals were divided into four groups, including 3 animals in each group. Animals were kept fasting overnight before the experiment, but water was given *ad libitum*. The animals were given an oral dose of 100 mg/kg of DMF and its cocrystals containing the same amount of DMF. Blood samples (0.25 ml) were isolated via retro-orbital under ether anaesthesia in the heparin-treated tube at 0.5 h, 1 h, 2 h, 4 h, 8 h, 12 h, and 24 h. Plasma was isolated

from blood samples by centrifuging the blood samples at 7000 rpm for 5 min at 4° C. The isolated plasma containing the drug (DMF) was extracted by precipitating it with an equal volume of acetonitrile. It was vortexed for a minute and centrifuged at 13000 rpm for 15 min. The clear supernatant was isolated and filtered at 0.22 µm for further HPLC analysis.

4.3.15 Statistical analysis

All values are expressed as the mean ± standard error mean (SEM). Two-way ANOVA followed by Bonferroni post-hoc test was performed to compare % sublimation at day-10 with day-20 and also to compare % cumulative dissolution rate at different time points for DMF and its cocrystals. One-way ANOVA followed by post-hoc student's Newman–Keuls test was performed for the analysis of all other biochemical parameters using Graph Pad Prism version 5 (San Diego, CA). Groups with $p < 0.05$ were considered significantly different. Various spectra were overlayed using Origin 2018. Pharmacokinetic data were analyzed using Kinetika5.0 software.

4.4 Result and discussion

4.4.1 Molecular docking

Molecular docking was used to identify the preferred poses of the interacting coformers of the SUCC and CIT with DMF. The numerous poses were generated using a Lamarckian genetic algorithm, which was then evaluated using AutoDock-4.2.6's semiempirical free energy force field-based scoring system. In the case of the CIT-DMF cocrystal, two hydrogen bonds between one of the oxygens contributed to the ester bond of the DMF and the hydrogens of the hydroxyl groups of CIT. Further, the lengths of hydrogen bonds were found to be 1.98 and 2.05 Å, with bond energies of -7.52 and -6.03 Kcal/mol. On the other hand, SUCC formed one hydrogen bond with DMF between the

esteratic oxygen of DMF and one of the hydroxyl groups connected to the carbonyl of SUCC. The bond length was found to be 2.12 Å and the bond energy of – 5.09 Kcal/mol (**Figure 4-2 and 4-3**).

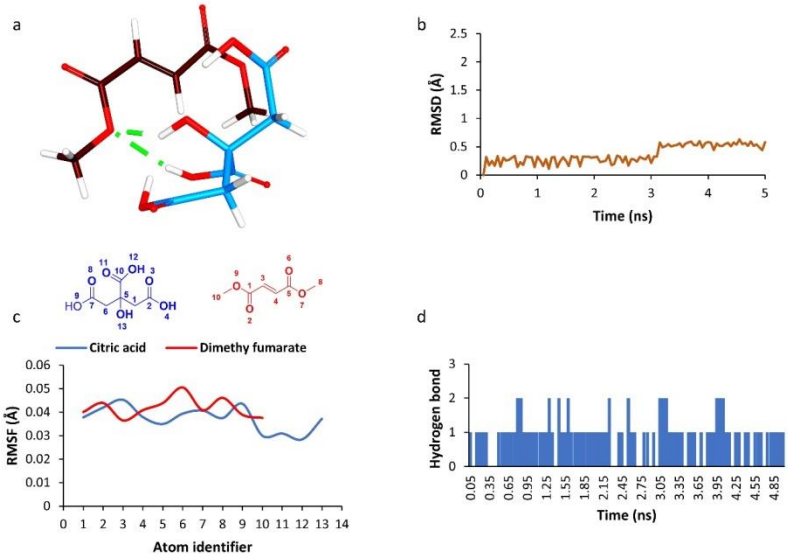

Figure 4-2 (a) 3D interaction between dimethyl fumarate and citric acid, (b) RMSD deviation of the system, (c) RMSF deviation of the atoms of dimethyl fumarate and citric acid, (d) Number of hydrogen bonds between dimethyl fumarate and citric acid w.r.t. time.

4.4.2 Molecular dynamics

The MD study was carried out using Amber20 to assess the stability of the interactions between the coformer units of the two cocrystals. A positional restrain force of 10000 Kcal/mol was applied to mimic the interstitial force experienced by the unit cell of a crystal [189]. Root mean square deviation (RMSD) displays the mean positional deviation of a group of atoms compared to a given frame. In the case of DMF-CIT cocrystal, it was observed that the RMSD was less than 1 Å, reflecting a state of stability. The mean RMSD was 0.366 ± 0.150 Å for the cocrystal, which was relatively less.

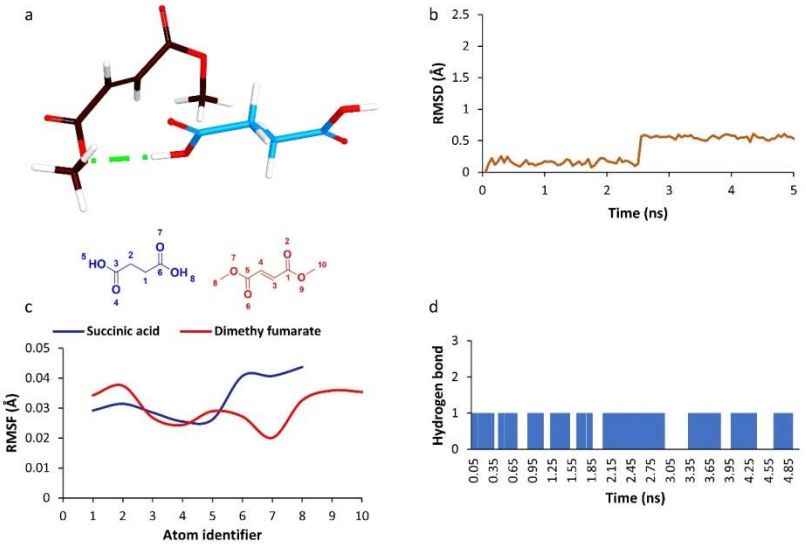

Figure 4-3 (a) 3D interaction between dimethyl fumarate and succinic acid, (b) RMSD deviation of the system, (c) RMSF deviation of the atoms of dimethyl fumarate and succinic acid, (d) Number of hydrogen bonds between dimethyl fumarate and succinic acid w.r.t. time.

Further, the fluctuation of a single atom could be measured using root mean square fluctuation (RMSF) for the entire simulation time. The RMSF of all the atoms of cocrystal was below 0.1 Å. The atoms, i.e., oxygen of the DMF and the hydroxyl oxygens of CIT displayed low RMSD, due to hydrogen bond formation. Further, one of the hydroxyl groups of CIT contributed towards hydrogen bond for 81 %, while the other contributed 19 % of simulation time **(Figure 4-2 and 4-3).**

The mean RMSD of CIT-DMF cocrystal was found to be 0.355 ± 0.205 Å, indicating a stable cocrystal. Further, the RMSF value for hydrogen bond forming atomic pair, i.e., esteratic oxygen of DMF and hydroxyl group of SUCC displayed a minimal fluctuation. Additionally, the hydrogen bond between the aforementioned pair was found to be for 72 % of simulation time.

4.4.3 Formulation of cocrystals

In this work, we considered that DMF would interact with its coformers- citric acid and succinic acid to form respective cocrystals in stoichiometric ratios. This would be facilitated by the interaction (as shown by FTIR spectra) of the carboxylic acid functional groups of citric acid and succinic acid with that of carbonyl groups of DMF. The probability of cocrystal formation was determined using the DSC cocrystal screening technique developed by [190]. The following parameters would ensure the cocrystallization of DMF with its various coformers.

4.4.4 Attenuated total reflectance FTIR (ATR- FTIR) spectroscopy

As shown in **Figure 4-4** spectrum, there was a shift in the carbonyl functional group in DMF-CIT cocrystal (1693 cm^{-1}) as compared to its pure DMF (1708 cm^{-1}) and citric acid (1679 cm^{-1})and their physical mixture (1702 cm^{-1}) respectively in their physical mixture to in the cocrystal formulation due to hydrogen bonding. New bonds were formed, showing broad peaks at 2800 cm^{-1} to 3200 cm^{-1} showing hydrogen bonding due to the interaction of carboxylic acid and the coformer.

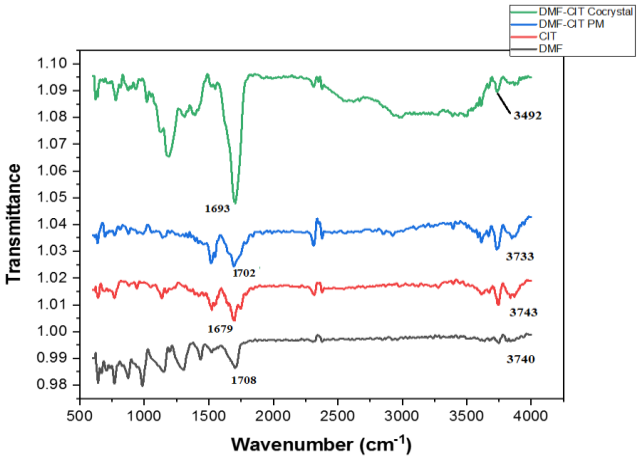

Figure 4-4 Showing IR spectra of DMF, citric acid, DMF-CIT physical mixture and DMF-CIT cocrystal.

As shown in **Figure 4-5**, there was a shift in the infra-red spectra of DMF-SUCC cocrystal 1691 cm^{-1} as compared to DMF spectra 1708 cm^{-1}. There was a broad peak in the cocrystal that appeared in the spectral range of 2800-3100 cm^{-1} respectively, which was not present in the drug or the coformer. The observed red-shift in the stretching modes of carbonyl, hydroxyl functional groups of DMF, CIT, and SUCC indicated the presence of hydrogen bonding interactions as well as the formation of cocrystals. Based on the changes in the frequency of the functional groups obtained in the ATR-FTIR of various cocrystals compared to the individual compounds and their physical mixtures, we ascertained the formation of novel solid forms.

A reduction of wavenumber by 251 cm^{-1} was observed. In the case of the carbonyl signal, there is a decrease of 15 cm^{-1} in wavenumber, as the signal was observed at 1708 and 1693 cm^{-1} for DMF and DMF-CIT co-crystal, respectively. Similar results were observed in DMF-SUCC cocrystals. This was found to be in agreement with the reference values provided [191, 192]. Hence clearly indicating the hydrogen bond between the moieties.

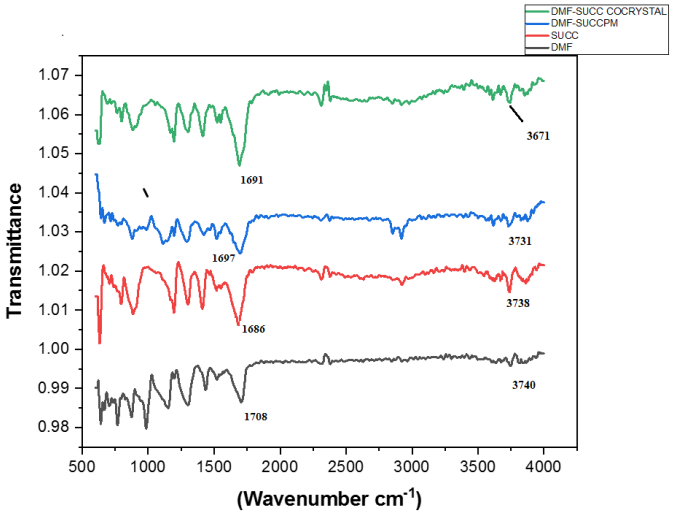

Figure 4-5 shows IR spectra of DMF, succinic acid, DMF-SUCC physical mixture and DMF-SUCC cocrystal.

4.4.5 Characterization of cocrystals by TGA

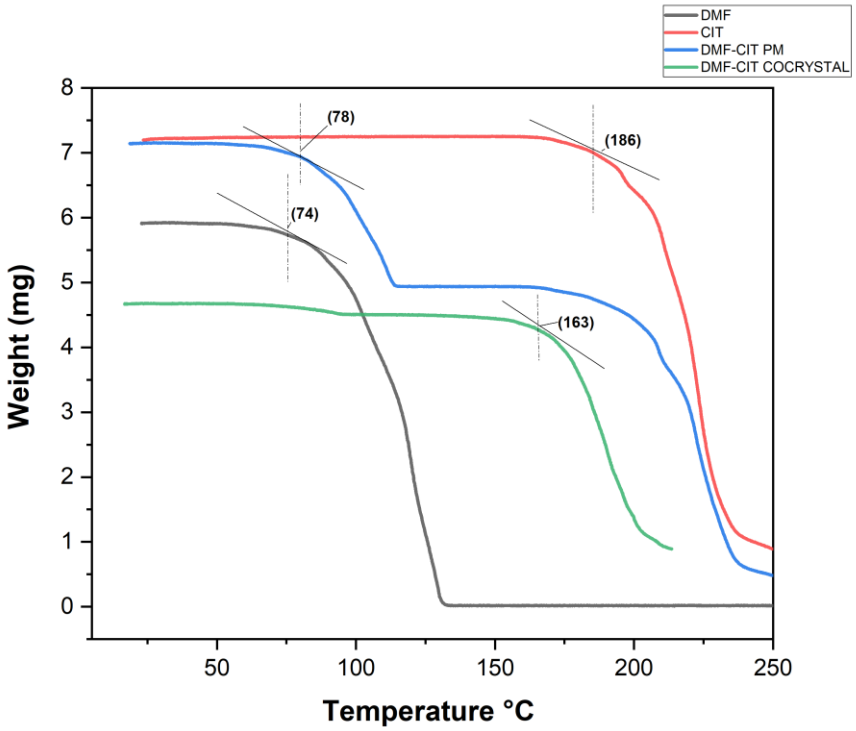

Figure 4-6 TGA thermogram of DMF, citric acid, DMF-CIT mixture and DMF-CIT cocrystal

A single-stage thermogram was obtained. T_{onset} for pure DMF was 74°C and for pure citric acid, it was 186°C. T_{onset} for DMF-CIT cocrystal was found at 163 °C with a single-stage thermogram.

As shown in **Figure 4-7** for the DMF-SUCC cocrystal, there was a two-staged thermogram. A two-stage thermogram is characteristic of many cocrystals which have been reported previously [153]. However, the weight loss due to decomposition up to T_{onset} was only 10.2% for cocrystal as compared with that of the physical mixture in which it was found to be 44.7%. Moreover, the thermogram for DMF-SUCC is not as well-differentiated as that of their physical mixture, signifying thermal protection. Earlier also, many have been utilizing succinic acid for making cocrystals for a long back, and it has been shown to provide physical and chemical stability to the API [193].

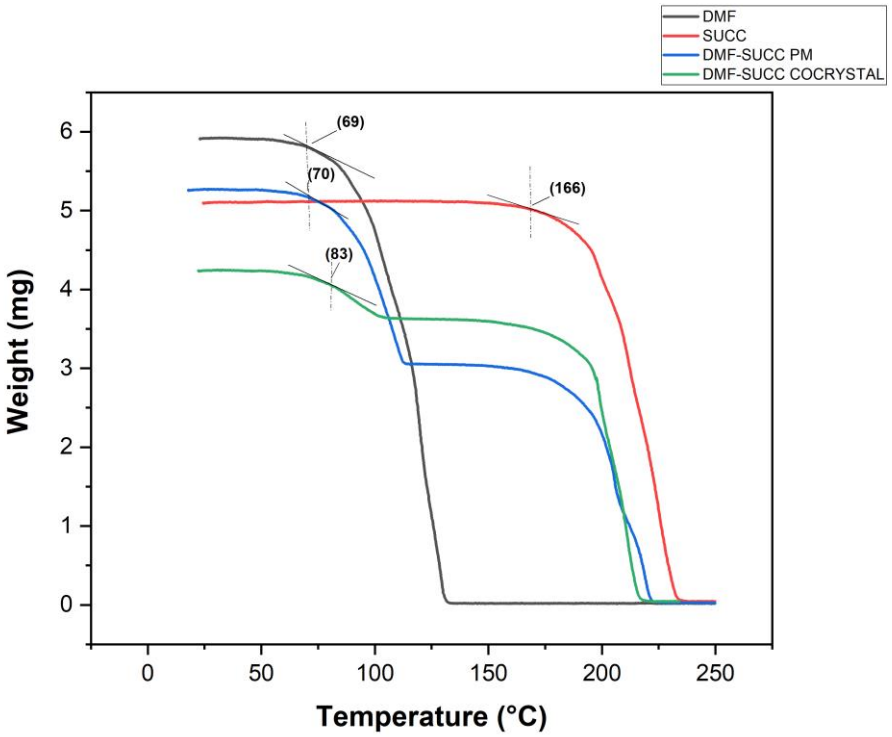

Figure 4-7 TGA thermogram of DMF, succinic acid, DMF-SUCC physical mixture and DMF-SUCC cocrystal.

From the obtained results, we found that pure components and the physical mixtures started losing their weight immediately when they reached their respective $T_{onset,}$ which represents their melting points. Still, there was an apparent shift in the T_{onset} in the case of cocrystals. Cocrystallization has brought thermostability to the thermolabile DMF for a higher temperature range. Previously also, cocrystals have been formulated to provide chemical and thermal stability to the active pharmaceutical ingredient [194].

4.4.6 Characterization of cocrystals by DSC

In **Figure 4-8**, endothermic peaks were obtained at 104°C and 156°C for DMF and CIT, respectively. We have found two sharp endothermic peaks at 104°C and 156°C for the physical mixture. A sharp endothermic peak at 148°C signifies cocrystallization and a broad peak obtained beyond 200°C signifies decomposition which is prominent in all the samples [195].

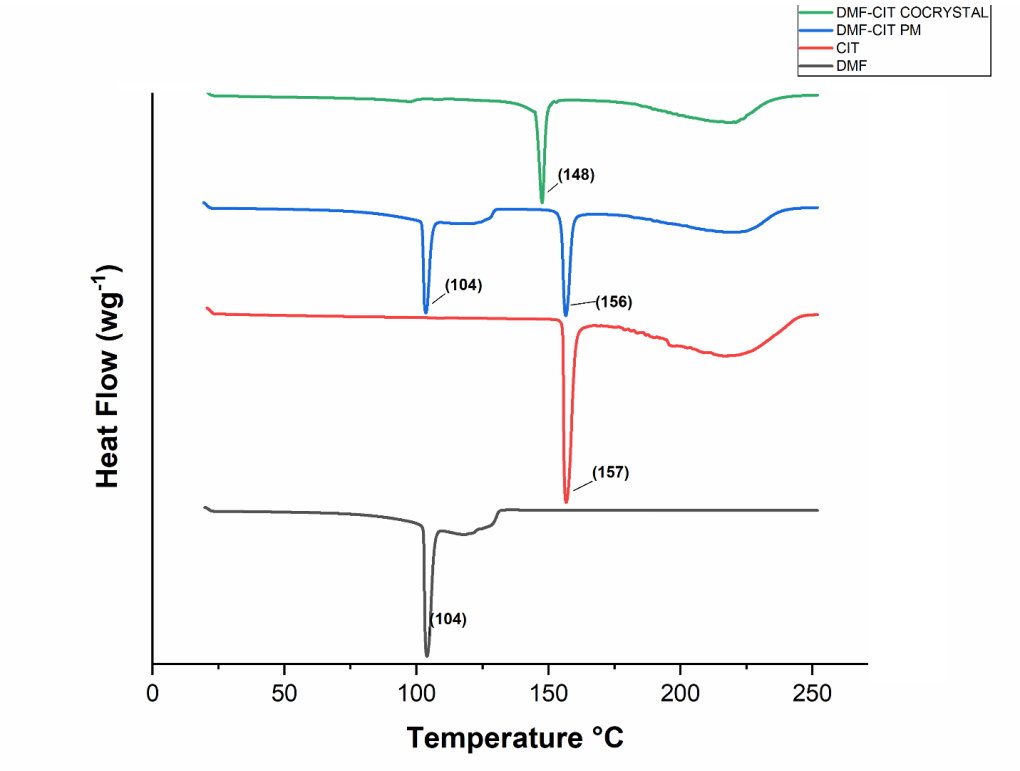

Figure 4-8 DSC thermogram of DMF, citric acid, DMF-CIT physical mixture and DMF-CIT cocrystal.

DMF-SUCC cocrystal as in **Figure 4-9,** shows shows two endothermic peaks at 112°C and 180°C but pure DMF and succinic acid showed endothermic peaks at 104°C and 189.3°C respectively. However, succinic acid has provided thermal stability to DMF in this experiment as well as in previous studies also [196].

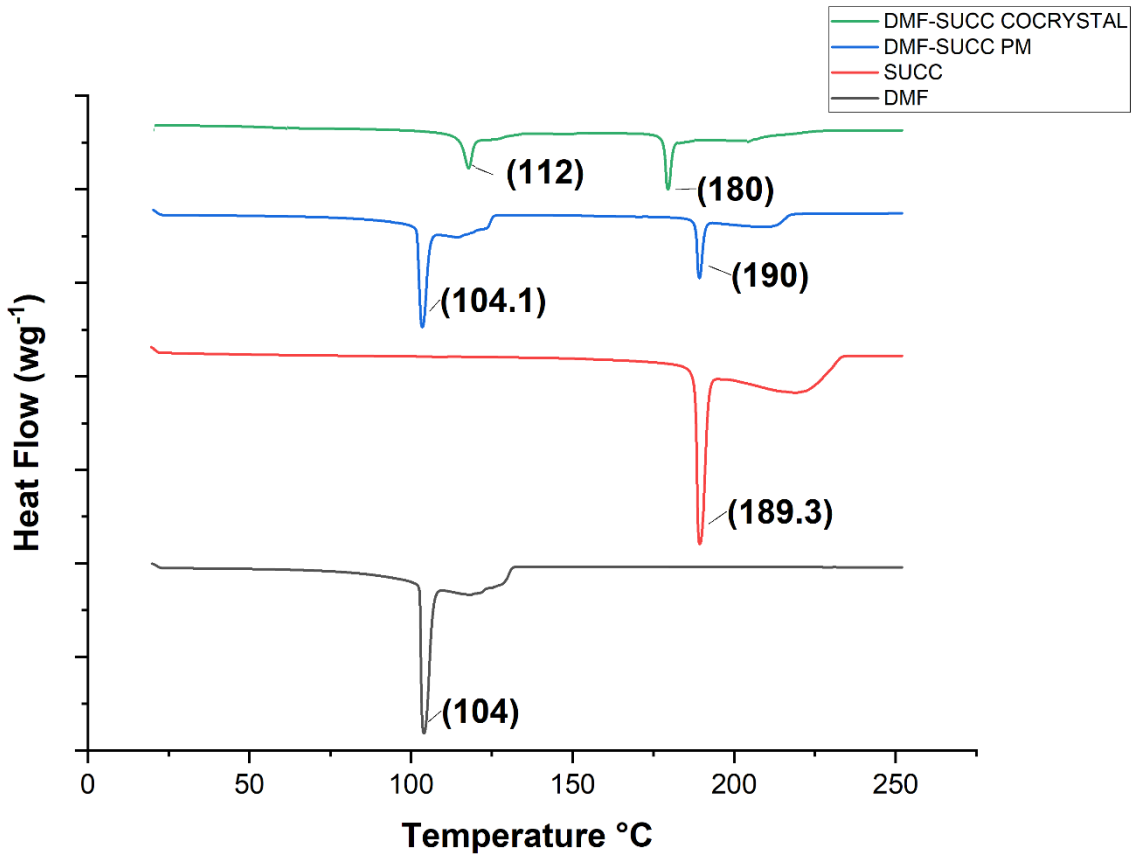

Figure 4-9 DSC thermogram of DMF, succinic acid, DMF-SUCC physical mixture and DMF-SUCC cocrystal.

The results showed that the melting points of API and coformers are proportional to the cocrystals. Coformers, CIT (153°C) and SUCC (188°C) with higher melting points gave cocrystal with high melting points DMF-CIT cocrystal, 148°C and DMF-SUCC cocrystal, 112°C and 180°C respectively. The coformers have provided thermal stability to DMF. Similar results were also observed in one of the studies in which the melting points of cocrystals were proportional to that of the coformers [173].

4.4.7 Characterization of cocrystals by PXRD

New peaks were obtained in the cocrystals as compared to their physical mixtures. With reference to the (**Figure. 4-10**), peaks disappeared in DMF-CIT PM at 2θ 11.1°, 14.26°, 15.53°, 17.5°, 19.56°, 22.14°, 24.22°, 25.08°, and 27.58° respectively, whereas new peaks

in DMF-CIT cocrystal;s appeared at 2θ 13.38°, 16.86°, 21.66°, 24.34°, 29.42° respectively.

As shown in **Figure 4-11**, for DMF-SUCC PM the peaks disappeared at 2θ 11.1°, 16.3°, 20.1°, 22.2°, 24.2°, 26.2°, 27.6 respectively contrary to this new peaks appeared in DMF-SUCC cocrystal at 2θ 12.5°, 16.7°, 18.8°, 20.8°, 22.5°, 23.2°, 25.5°, 26.8 and 27.8 respectively. Thus, all these significant changes in the cocrystals indicate cocrystallization.

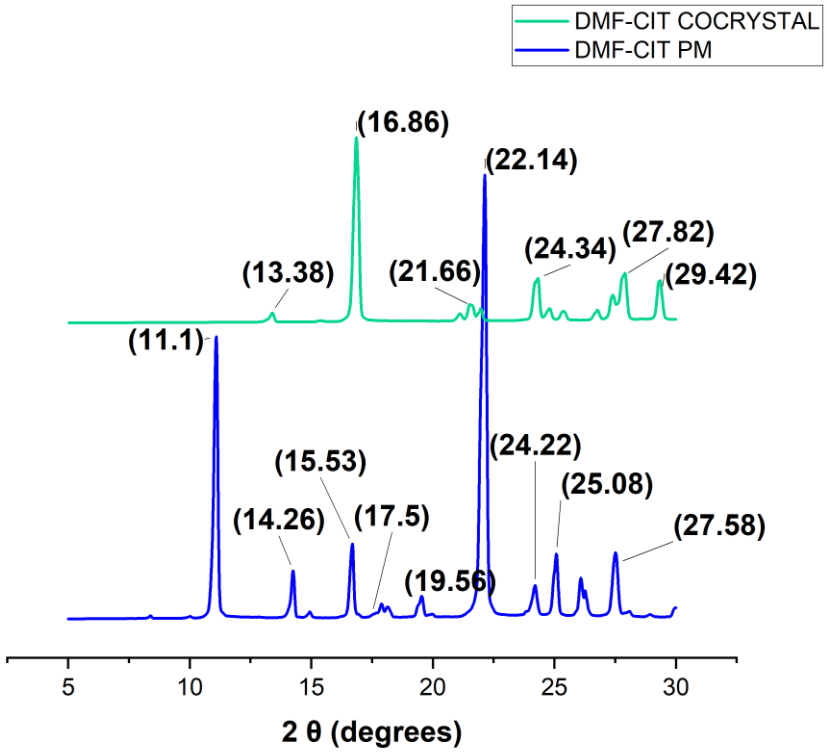

Figure 4-10 PXRD pattern of DMF, citric acid, DMF-CIT physical mixture and DMF-CIT cocrystal.

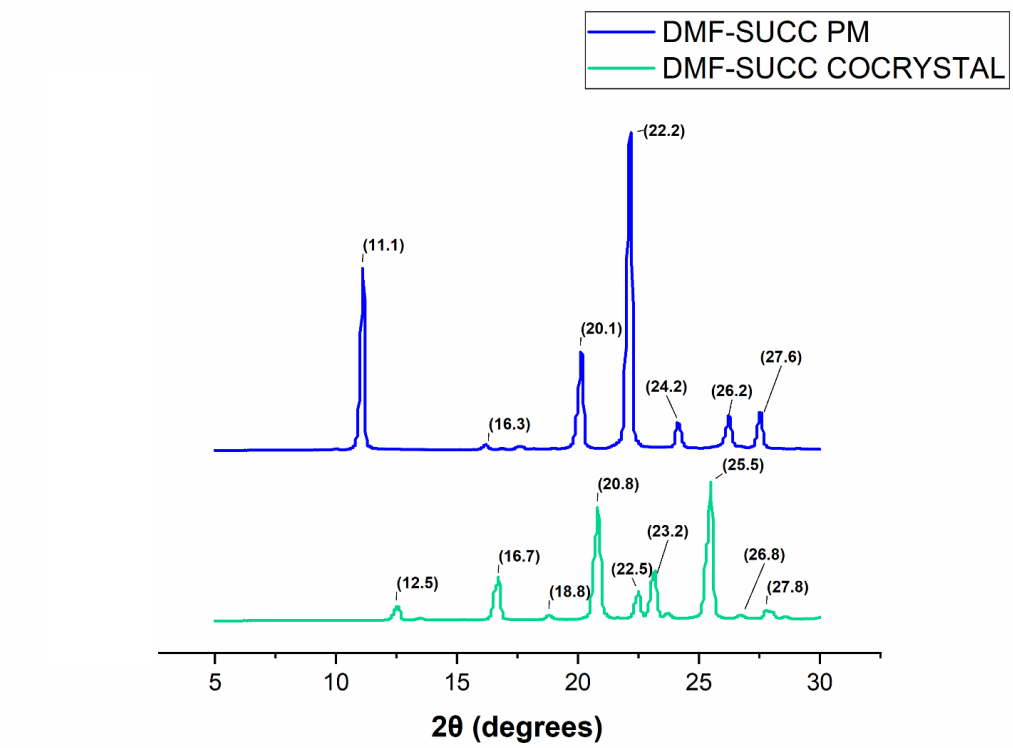

Figure 4-11 PXRD pattern of DMF, citric acid, DMF-CIT physical mixture and DMF-CIT cocrystal.

4.4.8 Effect of cocrystallization on sublimation behavior of DMF

We kept DMF, the two cocrystals, and their physical mixtures at 60°C, 75% RH maintained in an incubator for a duration of 20 days. Regarding the **Figure 4-12** shown below, statistical analysis using one-way ANOVA revealed a significant difference in % sublimed drug [$F(6, 28) = 313.9$, $p < 0.05$]. The post-hoc test revealed that cocrystallization decreased the sublimation of DMF significantly, as we can interpret from the result that percentage sublimation of DMF was 52.5% as compared to the cocrystals with % sublimation of 21.5%, and 17.5% for DMF-CIT, and DMF-SUCC respectively after day-10. We have found that after day-20, DMF had sublimed by 76.5% as compared to the cocrystals which had sublimed by 27%, and 34.3% for DMF-CIT, and DMF-SUCC respectively.

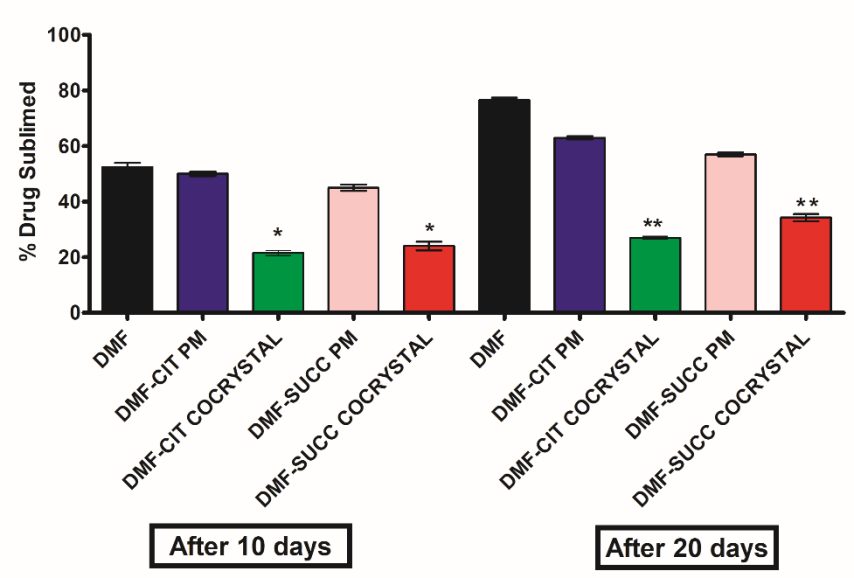

Figure 4-12 Showing sublimation of DMF, DMF-CIT cocrystal, and DMF-SUCC cocrystal over 20 days.

*All values are Mean ± SEM (n=3). *p< 0.05 compared to DMF at day-10 and **p< 0.05 compared to DMF at day-20 [one-way ANOVA followed by Newman-keuls test].*

4.4.9 Dissolution

The dissolution profiles of the prepared cocrystals were checked to quantify the rate of release of DMF as well as to check whether cocrystal formation has led to any change the release profile as shown in **Figure.4.13.** Two-way ANOVA revealed significant differences in % cumulative drug release among groups [F (3, 71) = 58.19, p <0.05], time [F (8, 71) = 601.0, p<0.05] and a significant interaction between groups and arms [F (4, 36) = 2.343, p<0.05]. Statistically, we have not found any change in the % cumulative drug release from DMF-SUCC when compared to DMF. However, in the case of DMF-CIT there was a decrease in the rate of % cumulative release at 15, 60, 75, 90 and 120 minutes respectively. The release rate of DMF-CIT was slower than the pure drug which can be seen in the **Figure.4-14** below. The probable reason can be the increased melting

point of the DMF-CIT which we have found to be more with respect to pure DMF since higher melting point leads to a decrease in the solubility [197].

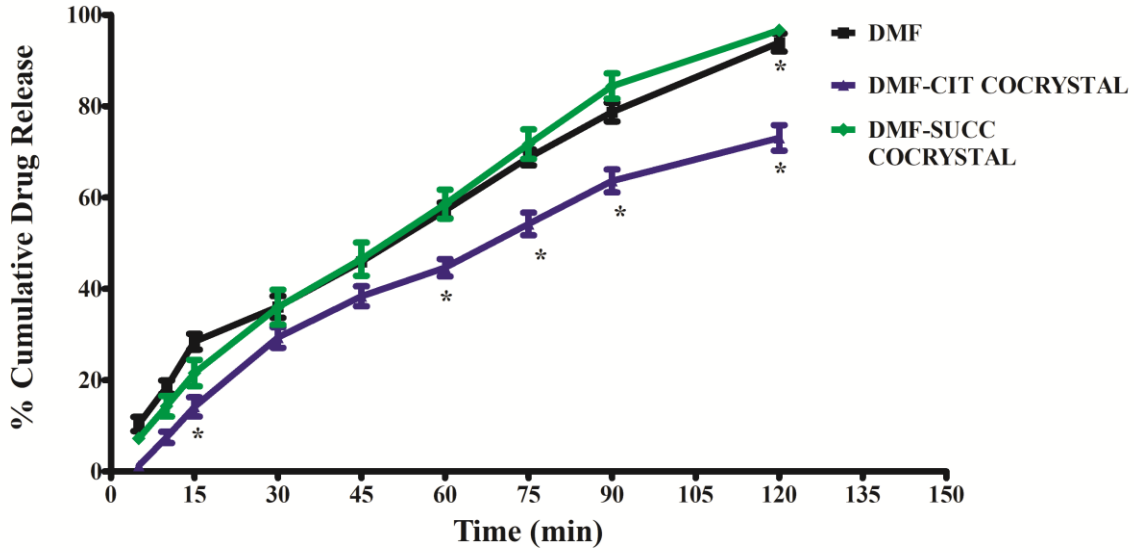

Figure 4-13 Shows % cumulative drug release with time for DMF, DMF-CIT cocrystal, and DMF-SUCC cocrystal.

All values are expressed as mean ± SEM (n=3) **).** **p< 0.05 compared to DMF [Two-way ANOVA followed by Bonferroni post-hoc test].*

4.4.10 Pharmacokinetics of DMF and its cocrystals

MMF which is the active metabolite of DMF was quantified using HPLC. Statistical analysis using one-way ANOVA had shown no significant difference among groups [F 3, 24) = 45.09, p < 0.05]**.** The post-hoc test revealed that the cocrystallization of DMF did not cause any change in the pharmacokinetic parameters. There was no statistical difference found whether it is the C_{max}, T_{max}, T_{half}, AUC and MRT among the various groups as shown in **Figure.4-14**.

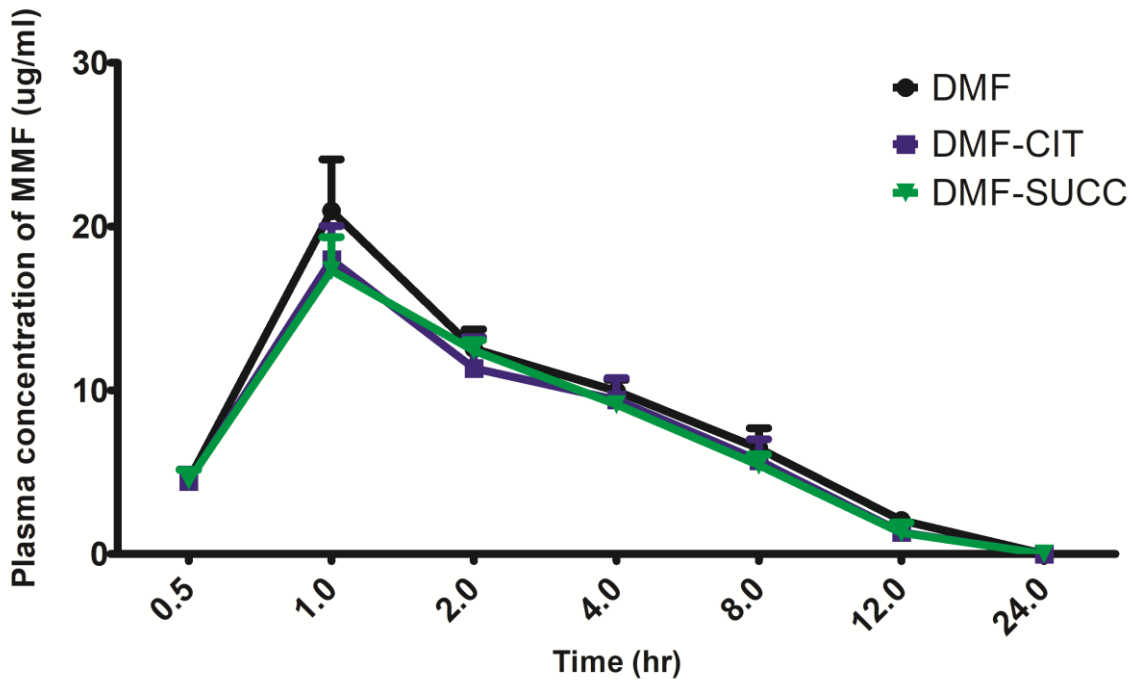

Figure 4-14 Showing plasma concentration of MMF over 24 hr after treatment of rats with DMF, DMF-CIT, and DMF-SUCC.

All values are expressed as mean ± SEM (n=3). [Two-way ANOVA followed by Bonferroni post-hoc test].

T**able 4 shows,** statistical analysis using unpaired t-test revealed no significant difference in the pharmacokinetic parameters like (C_{max}, T_{max}, $T_{1/2}$, MRT and AUC) of DMF and DMF-CIT cocrystal and DMF-SUCC cocrystal after oral administration.

Table 4 shows the pharmacokinetic parameters of DMF, DMF-CIT and DMF-SUCC cocrystals.

	DMF	DMF-CIT	DMF-SUCC
C_{max} (µg/ml)	20.954 ± 3.145	17.617± 2.070	16.789 ± 2.538
T_{max} (hr)	1.000 ± 0.000	1.000 ± 0.000	1.000 ± 0.000
$T_{1/2}$ (hr)	3.483 ± 0.294	3.361 ± 0.246	3.593 ± 0.188
MRT (hr)	5.676 ± 0.346	7.019 ± 1.832	7.273 ± 1.483
AUC (0-T) (µg*hr/ml)	106.500 ± 1.32	99.730 ± 1.115	110.270 ± 1.210

All values are expressed as mean ± SEM (n=3). [one-way ANOVA followed by Newman-Keuls Test].

4.4.11 Cell viability assay

Statistical analysis using one-way ANOVA had shown no significant difference among groups [F 3,8) = 2.006, $p < 0.05$]. The post-hoc test revealed that DMF and the two DMF cocrystals have no significant effect on the viability of the cells, as shown in the **Figure 4-15**. It signifies that the coformers and cocrystallization have not cause any toxic effects on the cells.

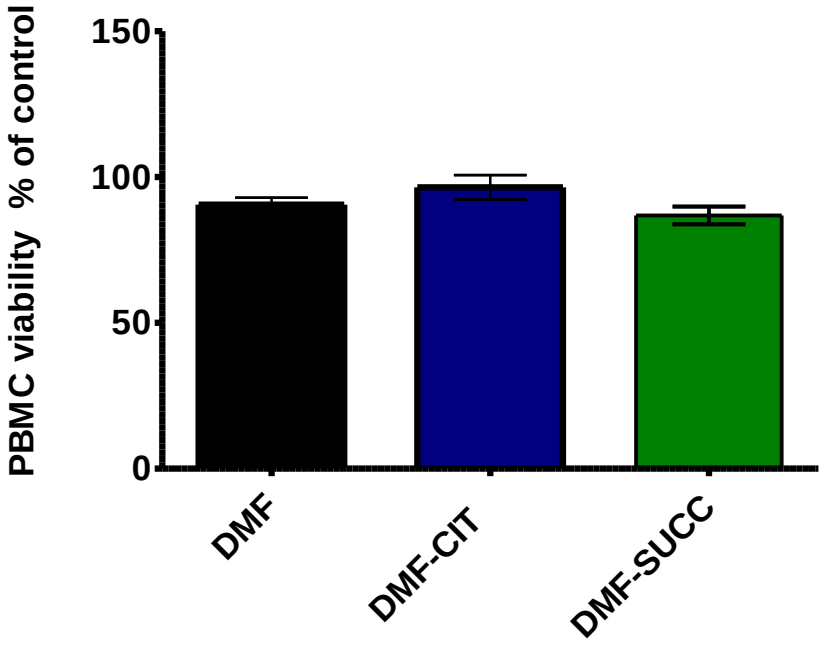

Figure 4-15 Showing cell viability assay of PBMC upon treatment with DMF, DMF-CIT cocrystal, and DMF-SUCC cocrystal.

All values are Mean ± SEM (n=4) [one-way ANOVA followed by Newman-keuls test].

4.4.12 ROS activity: DCF Assay

LPS induction to the immune cells causes a surge in intracellular reactive oxygen species (i-ROS) [198]. As shown in **Figure 4-16**, statistical analysis using one-way ANOVA showed a significant difference in ROS generation among groups [$F\ 4, 15) = 45.46$, $p < 0.05$]. The post-hoc test revealed that DMF and the two DMF cocrystals decreased the ROS concentration stimulated by LPS treatment to the PBMC significantly when compared with PBMC+vehicle and PBMC+LPS groups and the two cocrystals reduced ROS even more significantly than PBMC+LPS+DMF group.

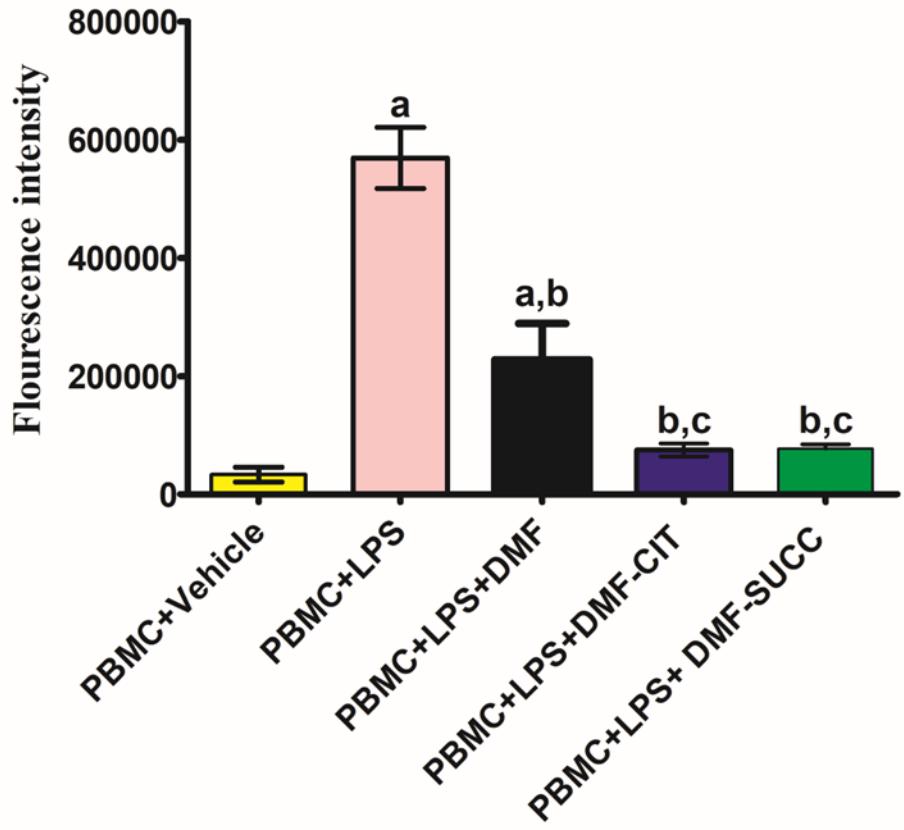

Figure 4-16 Showing fluorescence intensity due to i-ROS generation upon LPS induction and treatment with DMF, DMF-CIT, and DMF-SUCC in PBMC.

All values are Mean ± SEM (n=4). [a]p< 0.05 compared to PBMC+Vehicle, [b]p< 0.05 compared to PBMC+LPS, [c]p< 0.05 compared to PBMC+LPS+DMF [one-way ANOVA followed by Newman-keuls test].

4.4.13 Effect of cocrystals on IL-6 activity

To evaluate the anti-inflammatory effect of DMF, the immune cells need to be stimulated with the TLR4 agonist LPS which promotes cytokine release. LPS induction promotes the secretion of TNF, IL-6, IL-10, IL-13 and GM-CSF and DMF treatment is known to inhibit inflammatory cytokine-like IL-6 [199]. We have evaluated the effect of DMF and its cocrystals on IL-6 and it has been observed that LPS treatment to the PBMC brought

an increase in IL-6 production. As shown by **Figure 4-17** Statistical analysis using one-way ANOVA showed a significant difference in IL-6 production among the groups [F 4, 10) = 13.170, $p < 0.05$]. The post-hoc test revealed that cocrystallization of DMF and the two DMF cocrystals decreased IL-6 significantly, which has been stimulated by LPS treatment to the PBMC. Moreover, there was a significant difference between DMF and the DMF-cocrystals signifying the cocrystal's involvement in the inhibition of IL-6.

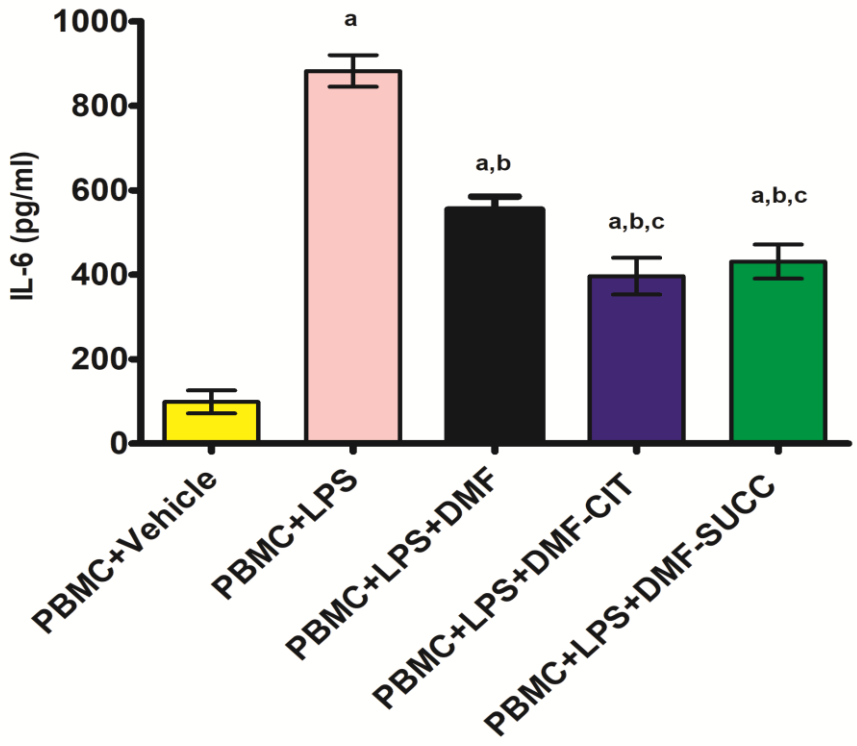

Figure 4-17 showing IL-6 activity upon LPS induction and treatment with DMF, DMF-CIT, and DMF-SUCC upon LPS induction in PBMC.

All values are Mean ± SEM (n=3) $^{a}p< 0.05$ compared to PBMC+Vehicle, $^{b}p< 0.05$ compared to PBMC+LPS, $^{c}p< 0.05$ compared to PBMC+LPS+DMF [one-way ANOVA followed by Newman-keuls test].

4.4.14 Effect of cocrystals on TNF-α activity

LPS induction to the immune cells is known to stimulate TNF-α release and DMF treatment has inhibited the level of cytokine TNF-α after LPS induction [200]. **Figure 4-18** shows the effect of DMF on LPS-induced TNF- α secretion on PBMC. We have found that LPS induction to the PBMC has stimulated TNF-α secretion and treatment with DMF and its cocrystals has attenuated the TNF-α level. Statistical analysis using one-way ANOVA showed significant differences in the TNF-α production among the groups [$F(4, 10) = 8.180$, $p < 0.05$]. The post-hoc test revealed that DMF and the two DMF cocrystals significantly decreased TNF-α which has been stimulated by LPS treatment to the PBMC and its production was further reduced by both the cocrystals significantly more than PBMC+LPS+DMF group.

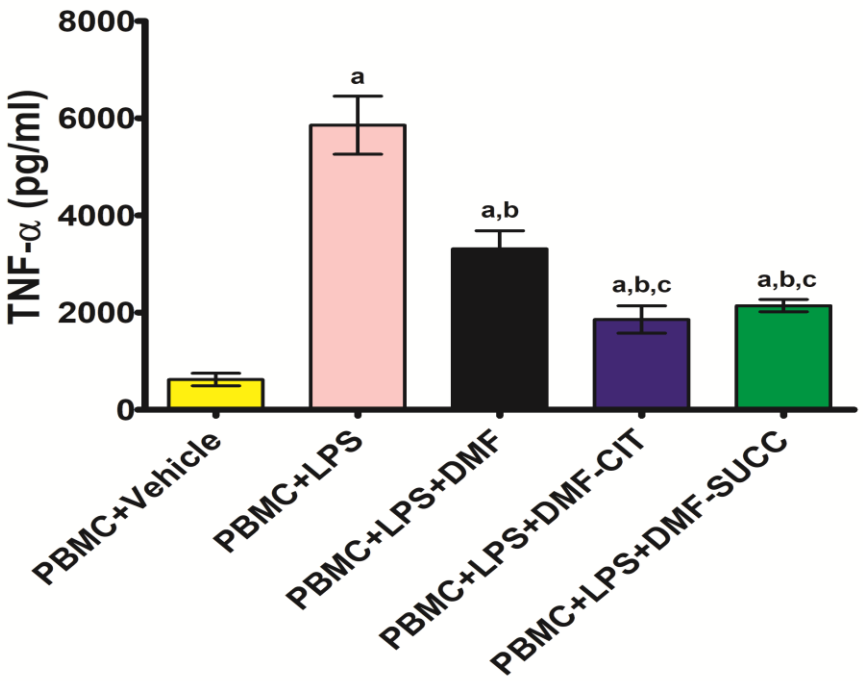

Figure 4-18 showing TNF-α activity on treatment with DMF, DMF-CIT, and DMF-SUCC upon LPS induction in PBMC.

All values are Mean ± SEM (n=3) [a]p< 0.05 compared to PBMC+Vehicle, [b]p< 0.05 compared to PBMC+LPS, [c]p< 0.05 compared to PBMC+LPS+DMF [one-way ANOVA followed by Newman-keuls test].

4.5 Discussion

The cocrystals have been utilized for various objectives like modulating bioavailability and physiochemical properties, we have formulated the cocrystals to provide thermal stability against sublimation. The coformers for the cocrystals have been selected based on molecular docking and dynamics-based computational studies [201]. The binding energy obtained in the molecular docking suggests interaction between the conformer and DMF which is necessary for cocrystal formation. Root mean square deviation (RMSD) is used to represent the mean positional deviation of a group of atoms compared to a given frame [202] as in **Figure 4-1** and **Figure 4-2**, is shown to be less than 1 reflecting a state

of stability between the coformers and the DMF. Concordant to RMSD, the lower value of Root mean square fluctuation (RMSF) defines the stability of individual atoms in the DMF and with respect to the coformrs, which in this experiment was found to be less than 0.1 A, therefore, conforming stability among the molecules [203].

Attenuated total reflectance FTIR (ATR-FTIR) spectroscopy has been utilized to find out physical interactions between the API and the coformers as there occur changes in the vibrational modes of the molecule when there occurs any hydrogen bonding or conformational change. It has been a familiar and reliable tool for characterizing cocrystals [204]. Cocrystallization is a result of interactions between different molecules that are present in the single-component crystalline phase [205]. Therefore, cocrystal formation can be confirmed by changes in the carbonyl frequencies of both pure DMF and its cocrystals as shown in **Figure 4-3.** and **Figure 4-4**.

Thermogravimetric analysis (TGA), differential thermal analysis (DTA) and differential scanning calorimetry (DSC) are important tools used for cocrystal characterization and for finding their properties [197].

TGA thermograms of the pure drug, the coformer and their physical mixture, and cocrystals prepared by various methods are shown in **Figure 4-5** and **Figure 4-6.** Usually, the thermal stability of a cocrystal is characterized by T_{onset}, which we have obtained from the intersection of the baseline weight and the tangent of the weight dependence on the temperature curve as decomposition occurs [206]. However, we have obtained that cocrystals have decomposed at much higher temperatures as compared to the DMF alone, which signifies thermal stability.

Melting point is one of the essential physical properties of solids, which is used to evaluate the purity of the product in which sharp melts signify purity and narrow ranges signify the presence of impurities. High melting point demonstrates the thermodynamic stability of the new materials, i.e. thermal stability of an API can be tailored by judicious selection of the coformers as found in our study shown in **Figure 4-7** and **Figure 4-8** Regardless of the methods used for the preparation of cocrystals, we have found many reports witnessing the application of differential scanning calorimetry (DSC) for a simple and rapid method to screen cocrystals [207].

Powder X-ray diffraction is considered a fingerprint characterization method for cocrystals. If the resulting PXRD of the solid product obtained after the cocrystallization experiment is different from that of the reactants, then it may be inferred that a new solid phase has formed [208]. Therefore, new peaks were obtained as shown in **Figure 4-9** and **Figure 4-10** signifying new solid phase with crystalline nature.

The cocrystals have been shown to overcome the process of sublimation significantly as shown in **Figure 4-11.** The thermal stability of the cocrystals can be further supported by the obtained TGA/DSC results as shown in the thermograms. The crystallization is known to provide stability against various physical stresses like thermal stress and thermal analysis is also essential to identify and understand the formation of cocrystals [209].

The cocrystals are known to alter the solubility and rate of dissolution of API based on its interaction with its coformers, including hydrogen bonding, solvent-solute interactions and ionization potential as discussed in the manuscript [210]. There was a decrease in the release rate of DMF-CIT cocrystal as shown in **Figure 4-12** which can be justified due to an altered melting point as a higher melting point leads to a decrease in the solubility of

the compound [197]. Cocrsyatlaization can alter the drug's pharmacokinetic parameters, as reported earlier [211]. However, we have not found any statistically significant changes in the pharmacokinetics profile upon cocrystalization, as shown in **Table 4 and Figure 4-13.** It signifies that there was no effect of cocrystalization on the parent DMF. Moreover, a correlation between *in-vitro* dissolution and *in-vivo* pharmacokinetics is expected, and we have obtained concurrence between the % cumulative release rate of the drug and pharmacokinetic parameters of DMF-SUCC. Still, in the case of DMF-CIT, we have found an anomaly, as explained above.

DMF is a known antioxidant drug. It has been shown to lower ROS concentration in many studies [212]. LPS has generated reactive oxygen species (ROS) in the PBMC, which was significantly reduced by DMF and its respective cocrystals, as shown in **Figure 4-14**. The two cocrystals have brought down the level of intracellular ROS more significantly as compared to the DMF. The additional anti-ROS activity in the cocrystals is due to the inherent antioxidant activity of the conformers [213].

DMF is known to have anti-inflammatory effects. In this experiment, cocrystals of DMF reduced the IL-6 and TNF-α even more significantly than DMF alone, as shown in **Figure 4-15** and **Figure 4-16,** respectively**.** The activity has been obtained due to the ability of DMF to block the induction of LPS-mediated suppression. This inhibition by DMF and cocrystal may be attributed to their action to inhibit nuclear factors like MAPK and NFκB, which activate inflammatory mediators in response to the TLR4 agonist LPS [199]. The obtained results open opportunities for using cocrytalisation a potential tool for modulating APIs for desired physicochemical and pharmacological properties.

4.6 Summary

We have prepared novel cocrystals of DMF using citric acid and succinic acid as coformers. Cocrystals have been formulated by using the solvent evaporation method and characterized by using spectral techniques of FTIR and diffractometry techniques of PXRD. The thermal evaluation has been done using TGA and DSC. Dissolution and pharmacokinetic studies compare the release profile of DMF with its cocrystal in *in-vitro* and *in-vivo* systems respectively. The cytotoxic and biological activity of DMF has been compared with that of the cocrystals. Cocrystals can be used as a potential tool to modulate the physicochemical and pharmacological characteristics of drugs.